Genetic analysis of a congenital split-hand/split-foot malformation 4 pedigree

XIAO YANG[1*], XINFU LIN[2,3*], YAOBIN ZHU[4*], JIEWEI LUO[2,5] and GENHUI LIN[2,6]

[1]Teaching and Research Office of Medical Cosmetology, Department of Management, Fujian Health College; [2]Provincial Clinical Medical College; [3]Department of Paediatrics, Fujian Provincial Hospital, Fujian Medical University, Fuzhou, Fujian 350001; [4]Department of Traditional Chinese Medicine, The First Affiliated Hospital, Fujian Medical University, Fuzhou, Fujian 350005; Departments of [5]Traditional Chinese Medicine and [6]Plastic Surgery, Fujian Provincial Hospital, Fujian Medical University, Fuzhou, Fujian 350001, P.R. China

Received January 2, 2018; Accepted February 22, 2018

DOI: 10.3892/mmr.2018.8838

Abstract. In the present study whole-exome sequencing using the Complete Genomics platform was employed to scan a proband from a split-hand/split-foot malformation (SHFM) 4 family. The missense mutation c.728G>A (p.Arg243Gln) in the *TP63* gene was revealed to be associated with SHFM. Sanger sequencing confirmed the sequences of the proband and his father. The father was diagnosed with SHFM and harbored a CGG-to-CAG mutation in exon 5, which produced a R243Q substitution in the zinc binding site and dimerization site of *TP63*. The R243Q mutation was predicted to be pathogenic by PolyPhen-2. The proband, who was diagnosed with four digit SHFM, exhibited a more severe phenotype. X-ray analysis returned the following results: Absence of third phalange bilaterally and third metacarpus of the left hand; absence of the second toes bilaterally and partial third toes; and partial fusion of the second, third and metatarsal bones of the right side with deformity of the second metatarsal of the right side. Osteochondroma was present in the fourth proximal radial metacarpal of the left hand and the basal and proximal parts of the second metatarsal of the right side. The proband's father had five digits in both feet. These results indicate that the R243Q mutation produces a novel phenotype named SHFM4. The present study revealed that the R243Q mutation in the TP63 gene produced a novel phenotype named SHFM4, thereby demonstrating the mutational overlap between ectrodactyly-ectodermal dysplasia-cleft syndrome and SHFM4.

Correspondence to: Dr Jiewei Luo, Department of Traditional Chinese Medicine, Fujian Provincial Hospital, Fujian Medical University, 134 Dongjie, Fuzhou, Fujian 350001, P.R. China
E-mail: docluo0421@aliyun.com

*Contributed equally

Key words: split-hand/split-foot malformation, ectrodactyly-ectodermal dysplasia-clefting syndrome, *TP63 (P63)*, mutation, pedigree

Introduction

Split-hand/split-foot malformation (SHFM) is a rare congenital limb defect with a wide phenotypic spectrum and high genetic heterogeneity. SHFM is primarily characterized by a deep median cleft of the hand and/or foot due to the poor differentiation of the apical ectodermal ridge (AER) during early embryonic development. Typical clinical manifestations include the following: ectrodactyly of the digits; presence of a wedge-shaped cleft on the palm (also known as crab-claw or lobster-claw anomaly); hypoplasia of the phalanges, metacarpals, and metatarsals; and polydactyly or syndactyly. Absence of the radial axis without cleft and monodactyly of the unaffected fifth digits have also been reported (1). To date, six different genetic loci of SHFM have been identified (2-6). Based on the different clinical manifestations of the affected organs, SHFM is classified as an isolated trait, as an asymptomatic disease (OMIM: 1863600), or part of a multiple congenital anomaly syndrome. Non-syndromic SHFM occurs as a sporadic deformity or as part of a syndrome associated with other limb defects, such as split-hand/foot malformation with long bone deficiency (SHFLD; OMIM: 119100), including tibial aplasia (7) (Table I). In general, the SHFM phenotypes of the different affected loci show no significant differences, making the genetic diagnosis of SHFM more challenging.

The *TP63* protein plays a significant role as a transcription factor involved in limb, epithelial, and craniofacial formation during the development of the mammalian embryonic endoderm (8). Approximately 10% of isolated SHFM4 cases are attributed to mutations in the human *TP63* gene. In addition, *TP63* mutations were detected in 93% of patients with ectrodactyly-ectodermal dysplasia-cleft (EEC) syndrome (9,10). All clinical conditions related to *TP63* mutations exhibit features that largely overlap with those of the EEC syndrome, thereby increasing the difficulty of diagnosis (11). In this study, we investigated the phenotype and genetic mechanisms underlying SHFM in a Chinese family with two members exhibiting isolated SHFM.

Subjects and methods

Clinical data of propositus and familial members. We performed whole-exome sequencing (WES) of proband (III3) using the Complete Genomics (CG) platform. Clinical data of propositus and familial members (Fig. 1), Clinical characteristics of the proband (III3) (Fig. 2A-D) are as follows. The proband is a 14-year-old male who was admitted to the hospital mainly because of deformities in both hands and feet for 12 years and camptodactyly of the second finger of the right hand for 11 years. Physical examination showed spinal physiological curvature without lateral bending. He was diagnosed with SHFM with only four digits in both hands and feet and with hands splitted into the ulnar and radial parts. Left hand fingers and bilateral toes functioned normally. Striated cicatricial contracture was observed in the 1st finger web and the second finger of the right hand, with camptodactyly of the second finger, a deep finger web between the separated 3rd and 4th metacarpal. X-ray results showed the absence of the 3rd phalange bilaterally and 3rd metacarpus of the left hand. The capitate of the left hand was significantly larger than that of the right hand, with the fourth proximal phalanx obviously expanded and formed a joint with the third and fourth metacarpals. Osteochondroma was present on the fourth proximal radial metacarpal of the left hand. The second toes were absent bilaterally, and only two sections of phalanxes of the third toes were present, which were accompanied by blurred and narrowed related metatarsophalangeal joint space. The second metatarsals of the left foot were smaller, especially the distal end, and was accompanied by deformity of the second metatarsal of the right foot. Osteochondroma was formed on the basal and proximal part of the second metatarsal of the right side, respectively. Pseudoarthrosis was present in the third metatarsal and the first phalanges, indicating deformity of both hands and feet with partial bone dysplasia.

Clinical manifestations of (II3) are as follows (Fig. 2D and F). The proband was diagnosed with SHFM and had five digits in both feet. X-ray results showed that the proximal joints of the second toe of the right side was buckling and fused with the soft tissue of the first toe. In addition, the first and second toes of the left foot were separated. The proximal soft tissues of the second to fourth toes of the left foot were fused. The second, third, and fourth distal soft tissues of the left foot were separated. The rest of the bone cortex was intact and showed continuous trabecular bone. There were no obvious abnormalities in bone structure, joint relationship, and shapes of the hand and hand joints. The two patients and their family members did not exhibit deafness, mental retardation, and external body malformations, such as face, palate, anadontia, and other obvious deformities.

DNA extraction. Genomic DNA was extracted from peripheral blood samples (QIAamp DNA Blood Mini kit; Qiagen, Hilden, Germany). The concentration and purity of the DNA extracts were determined using a NanoDrop 1000 instrument (Nanodrop Technologies; Thermo Fisher Scientific, Inc., Pittsburgh, PA, USA). All procedures were performed in accordance to the tenets of the Declaration of Helsinki and approved by the Ethics Committee of Fujian Provincial Hospital (Fuzhou, China). All participants and legal guardians of the minors involved in the present study provided written informed consent.

CG whole exome sequencing. The proband (III3) was examined via WES using the CG platform (Complete Genomics, Inc., San Jose, CA, USA) for next generation sequencing (NGS). First, Covaris was used to randomly fragment the genomic DNA (gDNA). Fragments ranging from 200 to 400 bp were selected after two rounds of bead purification. Next, the AdA 5'- and 3'-adaptors were ligated to the 5'- and 3'-ends of the fragments, respectively, before PCR amplification. The PCR products were then subjected to exon capture. Captured exon fragments were purified via DynabeadsM-280 Streptavidin Bead purification and further amplified by another round of PCR. The products were cyclized to generate double-strand (ds) circles, which were digested with Ecop15I. Small fragments were collected after bead purification. Following the same procedure as in AdA adaptor ligation, AdB adaptors were also ligated to both ends of the purified fragments. The fragments then underwent single-strand (ss) cyclization. The resulting ss circles were used as the final library products for sequencing on the CG Black Bird platform. Finally, high-throughput sequencing was performed for each captured library to ensure that each sample meets the desired average sequencing depth.

Bioinformatics analysis. After base calling, reads sequence of each DNA nano-balls (DNBs) are derived. Initial mapping is conducted by an in-house mapping tool, Teramap, developed by Complete Genomics, Inc.. Based on the initial mapping results, the regions which are deemed to differ from the reference genome are identified. Then individual reads that lie in those regions are chosen to perform a local de novo assembly. The assembly results are converted together with the initial mapping into a BAM file which only includes mapped reads. Next according to the initial mapping and the assembly results, a probability statistical model is adopted to acquire variants. Variants extracted from the model with a probability higher than a significant threshold are reported. Finally, small variants with high confidence are selected and annotated. A strict data analysis quality control system (QC) is built throughout the whole analysis (12-14).

Sanger DNA sequencing. Variants were confirmed using Sanger DNA sequencing in this family (I2, II1-4 and III1-3). Primers for amplification of the target sequences were designed using Premier 5 software and synthesized by Thermo Fisher Scientific, Inc. (Shanghai, China). The *TP*63 gene sequence was obtained from GenBank (NM_003722.4), and the length of the target sequence was 226 bp and the primers were synthesized by Thermo Fisher Scientific, Inc. The following primer sequences were used for amplification: *TP*63-F: 5'-GACATG CCCCATCCAGATCAA-3' and *TP63*-R: 5'-AGGTGGGTC TCAAACAAAAATGC-3'. PCR products were purified using the Omega E.Z.N.A.™ Gel Extraction kit (Omega Bio-tek, Norcross, GA, USA) according to the manufacturer's instructions. Sanger sequencing was performed using the BigDye Terminator v1.1 kit following the manufacturer's instructions and on a 3730xl DNA Analyzer (Thermo Fisher Scientific Inc.).

Results

Statistics of whole exome sequencing. WES of one DNA sample produced an average of 503,436,416 DNBs using the CG

Table I. Human genetic mapping of SHFM and SHFLD.

Phenotype	Omim database number	Location	Gene/locus	Mode of inheritance
SHFM1	OMIM 183,600	7q21	*DLX5, DLX6, DSS1*	Autosomal dominant
SHFM2	OMIM 246,560	Xq26	*FGF13*	X-linked recessive
SHFM3	OMIM 246,560	10q24	*HOX11, FGF8*	Autosomal dominant
SHFM4	OMIM 605,289	3q27	*TP63 (p63),*	Autosomal dominant
SHFM5	OMIM 606,708	2q31	*HOXD13*	Autosomal dominant
SHFM6	OMIM 183,600	12q13	*WNT10b*	Autosomal recessive
SHFLD1	OMIM 119,100	1q42.2-q43		Autosomal dominant
SHFLD2	OMIM 610685	6q14.1		Autosomal dominant
SHFLD3	OMIM 612,576	17p13.3	*BHLHA9*	Autosomal dominant

SHFM, split-hand/foot malformation; SHFLD, SHFM with long bone deficiency.

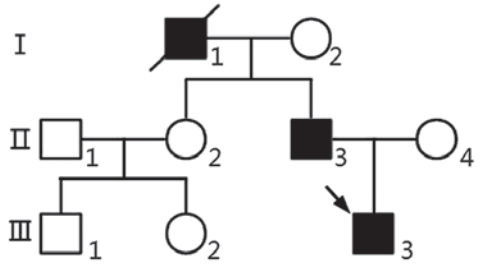

Figure 1. Pedigree chart of the Chinese split-hand/split-foot malformation 4 family. The arrow indicates the proband. Squares represent males, while circles represent females. The shaded circle represents the patient. I, 1st generation, II, 2nd generation, III, 3rd generation. The numbers indicate the membership number of each generation.

platform. Duplicate DNBs, DNBs with too many good reference mappings, and DNBs with no consistent mate mappings were filtered out prior to variant calling. After filtering, a total of 475,501,541 DNBs were used as input for local *de novo* assembly and variant detection. In this study, 58.97-Mb target regions were captured, and an average of 11.56 GB of mapped bases were generated per individual. On average, 99.53% of the target bases were sequenced with at least 1X coverage per sample, and 97.34% of the bases were sequenced with at least 10X coverage per sample.

A total of 43,846 SNPs were identified in all individuals. Furthermore, 97.37% of all variants were represented in dbSNP, while 95.64% were annotated in the 1000 Genomes Project database. We identified 755 novel SNPs with a transition-to-transversion ratio of 2.61. Of all SNPs, 10,280 were synonymous mutations, while 9,442 were missense mutations. A total of 34 SNPs were stop-loss, 66 stop-gain, and 16 start-loss mutations. In addition, 65 SNPs were located in splice sites.

A total of 3,591 indels were identified in all samples. Of these, 80.76% were represented in dbSNP and 66.33% were annotated in the 1000 Genome Project database. The analysis identified 608 novel indels. Of all the indels, 178 were frameshift, three were stop-loss, three were start-loss, and 44 were splice-site mutations. A total of 1,702 point mutations had maf ≤1%, which included 1,056 amino acid substitutions and splice mutations and 107 indel mutations.

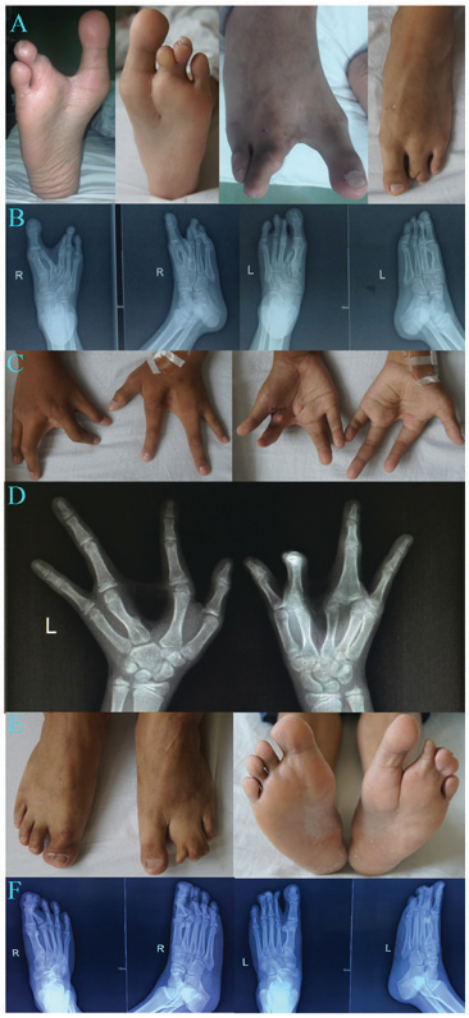

Figure 2. Clinical and X-ray images of patients from the split-hand/split-foot malformation 4 family. (A-D) The proband. (E and F) The father of the proband. L, left; R, right.

Determination of suspected pathogenic mutations in the propositus. The DNBs of each sample were compared with the reference human genome sequence (GRCh37/HG19). Based on the candidate genes listed in Table I, we performed direct screening to identify putative mutation sites. The c.728G>A

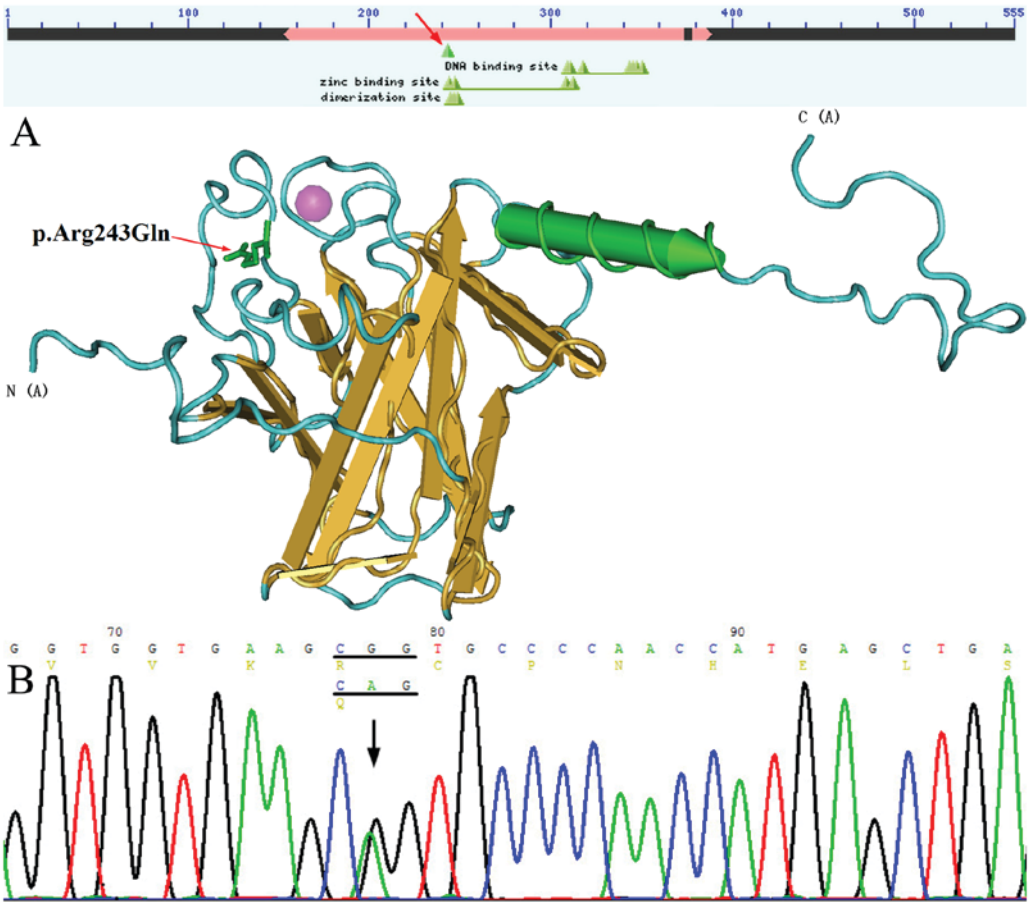

Figure 3. Mutations in patients from the split-hand/split-foot malformation 4 family. (A) The three-dimensional structure of the *TP63* protein. Arg243Gln is located in the zinc binding site and dimerization site of *TP63*. (B) The sequencing map of the c.728G>A (p.Arg243Gln) of *TP63*.

(p.Arg243Gln) (rs121908836) mutation located within *TP63* was detected in the proband (III3) and his father (II3), who was diagnosed with SHFM. A CGG-to-CAG mutation (c.728G>A) in exon 5 predicted an arginine-to-glutamine substitution at amino acid position 243 (R243Q), which is located in the zinc binding site and dimerization site of *TP63* (15,16) (Fig. 3). This missense variant was predicted to be pathogenic by PolyPhen-2 and was not detected in other family members. In addition, a synonymous variant, c.1059C>T (p.His353His)/(rs1051886), was identified in the candidate gene *WNT10b* of the proband.

Discussion

SHFM disorders are highly heterogeneous and exhibit variable clinical manifestations, which are attributed to multiple loci and various inheritance modes. *TP63* is an important functional gene that is involved in tissue development and apoptosis. Mutations in human *TP63* can lead to developmental disorders, including the EEC syndrome, ankyloblepharon-ectodermal defects-cleft lip/palate syndrome (AEC), limb-mammary syndrome (LMS), acro-derma-to-ungual-lacrimal-tooth syndrome (ADULT), Rapp-Hodgkin syndrome (RHS), SHFM4, and nonsyndromic cleft lip (NSCL) (17). Similarly, previous studies have reported that EEC syndrome in a small number of families were caused by a p.Arg243Gln mutation in *TP63* (5,9). We first discovered the isolated SHFM4 genetic phenotype corresponding to this point mutation, which is characterized by congenital ectrodactyly, syndactyly, without prosopo-cleft, and ectodermal dysplasia.

The majority of EEC syndrome cases are caused by a missense mutation in the core DNA binding domain (DBD) of *TP63*, thereby disrupting its ability to translate proteins normally. On the other hand, only 10% of the nonsyndromic SHFM cases are attributed to *TP63* mutations. Mutations in the domain of the *TP63* gene can lead to isolated/nonsyndromic SHFM but also result in syndrome SHFM, which indicated that morphological classification may not be reliable for accurate diagnosis (1). The mutation spectrum of the EEC syndrome reflects a specific pathogenetic mechanism. Several studies have provided strong evidence that codons 204, 279, 280, and 304, could result in both EEC and SHFM (5,18). Mutations in codon 204 are consistent with our current results showing the effects of the R243Q mutation (rs121908836, NM_003722.4). The above findings demonstrate the partial overlap between the mutational spectra of EEC and SHFM. ADULT and EEC are generally caused by missense mutations in the DBD, whereas AEC and LM syndromes are caused by missense mutations in the SAM region and in other nearby regions. SHFM is caused by mutations in various regions of *TP63*. Different mutations have been shown to result in different effects, indicating that *TP63* is involved in various developmental functions (8,9). So far, p.Arg97Cys, p.Lys233Glu, and p.Arg319Cys mutations in *TP63* were identified in isolated SHFM4 patients (19,20). The p.Arg97Cys and p.Lys233Glu

mutations occur in the N-terminal transactivation domain (TA) domain, whereas p.Arg319Cys mutations are found in DBD loci. The Human Gene Mutation Database (HGMD) reported that missense variants in position 243 (R243Q, R243W, and R243L) and in nearby residues (V241M, H247Y, H247D, and H247R) are associated with *TP63*-related disorders, thereby supporting the functional importance of this *TP63* region. The most common phenotypes of patients harboring mutations in position R243 include hair, lacrimal duct, and nail defects, which can be observed in the EEC3 syndrome (604292) (21).

All amino acids of p53 that directly bind DNA are conserved in both *TP63* and p73. The transcription factors *TP*63 and p73 belong to the p53 family and have been predicted to perform similar functions. The human *TP63* gene is located in the 3q27-3q29 chromosomal region, which encodes specific domains (22,23), including the TA domain, DBD, and oligomerization domain (OD). Unlike p53, *TP63* contains a unique N-terminal SAM (sterile alpha motif) region, which is also found in many signaling proteins involved in cell development and differentiation (24,25).

P73 and *TP63* encode various homologs which differ based on the carboxyl termini. In particular, the α, β, and γ isoforms exhibit diverse biological characteristics (22). Under the influence of the P1 and P2 promoters, *P73* and *TP63* respectively transcribe two isomers, namely, Tap73/63, which contains the TA region, and the N-terminal truncated isomer ΔNp73/63. These two proteins have opposing biological characteristics; Tap73/63 promotes p53 function, whereas ΔNp73/63 antagonizes p53 function (26). The zinc binding site and dimerization site are located in the TA region. The TAp63 subtype can induce developmental cell apoptosis. p53, p*TP63*, and p73 are involved in similar but distinct physiological processes. *P53*-knockout mice may exhibit high frequency of spontaneous tumors during development. The active p53 protein does not participate in physiological apoptosis during the entire embryonic development process, whereas *TP63*- and *P73*-knockout mice exhibit specific limb and epithelial developmental malformations without inducing the formation of spontaneous tumors (27).

ΔNp63 subtypes are primarily expressed in late embryos and during postnatal epidermal development. The gene knockout mouse model demonstrated that the ΔNp63 protein is essential for maintaining the integrity of the epidermal basal layer, final differentiation of keratinocytes, and initial stratification of the epithelium during embryonic development (28,29). These processes can be induced by activation of the ΔNp63 gene during epidermal differentiation. The ΔNp63 mutation not only determines ectodermal fate, but also influences ectodermal embryonic stem cell proliferation and epidermal formation, which are important in maintaining the proliferation potential of epidermal stem cells in the mature epithelium (30). In *TP63*-deficient mice, multiple layers of regenerated epithelial stem cells can be inactivated and can undergo asymmetric division (31). Knockout mice overexpress ΔNp63α in the skin, which leads to characteristic changes, such as delayed wound healing, reduced skin thickness, decreased subcutaneous adipose tissue, hair loss, reduced cell proliferation, and accelerated skin aging, some of which can be ameliorated by Sirt1 regulation (32).

The p.R243Q mutation in the TA region affects the binding of zinc ions, which can lead to incorrect folding of the protein and impair tap63 function. In turn, reduced tap63 function leads to ΔNp63 overexpression, which inhibits apoptosis by downregulating the expression of pro-apoptotic genes (33) and ultimately affects the development of the epidermis. In addition, SHFM can produce the ectrodactyly phenotype and mainly effects the development of central rays of the autopod. The most common cause of SHFM is interference in the AER signaling pathway. Reduced AER signaling promotes AER cell death or inhibits cell proliferation. As a result, the activity of central AER cannot be maintained, which directly causes distal limb defects. AER abnormalities occur during limb development (34,35).

A few studies have reported the role of *TP63* in SHFM, and some case reports have implicated mutations in the zinc binding site of *TP63* in SHFM. In the present study, we demonstrated that the R243Q mutation in the *TP63* gene produces a new phenotype called SHFM4, thereby demonstrating the mutational overlap between EEC and SHFM4. The genetic and clinical heterogeneity of SHFM significantly increases the difficulty of genetic counseling. Therefore, identifying the genetic alterations that are responsible for SHFM in individual patients is of practical importance.

Acknowledgements

Not applicable.

Funding

This study was supported by grants from the Financial Scheme for Young Talents Training Program of Fujian Health industry (grant no. 2015-ZQN-ZD-7), Fujian Provincial Natural Science Fund Project (grant no. 2016J01501) and Fujian Provincial Health and Family Planning Youth Research Program, China (grant no. 2016-1-84).

Availability of data and materials

The datasets used and/or analyzed during the current study are available from the corresponding author on reasonable request.

Authors' contributions

JL conceived and designed the study and drafted the manuscript. XY, XL, YZ and GL performed the data collection, statistical analyses and drafted the manuscript. The final version of the manuscript was read and approved by all authors.

Ethics approval and consent to participate

All procedures were performed in accordance to the tenets of the Declaration of Helsinki and the study was approved by the Ethics Committee of Fujian Provincial Hospital (Fuzhou, China). All participants and legal guardians of the minors involved in the present study provided written informed consent.

Consent for publication

Written informed consent was obtained for the publication of the participants data and clinical images.

Competing interests

The authors declare that they have no competing interests.

References

1. Basel D, Kilpatrick MW and Tsipouras P: The expanding panorama of split hand foot malformation. Am J Med Genet A 140: 1359-1365, 2006.
2. Duijf PH, van Bokhoven H and Brunner HG: Pathogenesis of split-hand/split-foot malformation. Hum Mol Genet 12: R51-R60, 2003.
3. Amalnath SD, Gopalakrishnan M and Dutta TK: Split-hand/feet malformation in three tamilian families and review of the reports from India. Indian J Hum Genet 20: 92-95, 2014.
4. Klar AJ: Split hand/foot malformation genetics supports the chromosome 7 copy segregation mechanism for human limb development. Philos Trans R Soc Lond B Biol Sci 371: 20150415, 2016.
5. Celli J, Duijf P, Hamel BC, Bamshad M, Kramer B, Smits AP, Newbury-Ecob R, Hennekam RC, Van Buggenhout G, van Haeringen A, *et al*: Heterozygous germline mutations in the p53 homolog p63 are the cause of EEC syndrome. Cell 99: 143-153, 1999.
6. Khan S, Basit S, Zimri FK, Ali N, Ali G, Ansar M and Ahmad W: A novel homozygous missense mutation in WNT10B in familial split-hand/foot malformation. Clin Genet 82: 48-55, 2012.
7. Armour CM, Bulman DE, Jarinova O, Rogers RC, Clarkson KB, DuPont BR, Dwivedi A, Bartel FO, McDonell L, Schwartz CE, *et al*: 17p13.3 microduplications are associated with split-hand/foot malformation and long-bone deficiency (SHFLD). Eur J Hum Genet 19: 1144-1151, 2011.
8. Van Bokhoven H, Melino G, Candi E and Declercq W: p63, a story of mice and men. J Invest Dermatol 131: 1196-1207, 2011.
9. van Bokhoven H, Hamel BC, Bamshad M, Sangiorgi E, Gurrieri F, Duijf PH, Vanmolkot KR, van Beusekom E, van Beersum SE, Celli J, *et al*: p63 Gene mutations in EEC syndrome, limb-mammary syndrome and isolated split hand-split foot malformation suggest a genotype-phenotype correlation. Am J Hum Genet 69: 481-492, 2001.
10. Sowińska-Seidler A, Socha M and Jamsheer A: Split-hand/foot malformation-molecular cause and implications in genetic counseling. J Appl Genet 55: 105-115, 2014.
11. Celik TH, Buyukcam A, Simsek-Kiper PO, Utine GE, Ersoy-Evans S, Korkmaz A, Yntema HG, Bodugroglu K and Yurdakok M: A newborn with overlapping features of AEC and EEC syndromes. Am J Med Genet A 155A: 3100-3103, 2011.
12. Robinson JT, Thorvaldsdóttir H, Winckler W, Guttman M, Lander ES, Getz G and Mesirov JP: Integrative genomics viewer. Nat Biotechnol 29: 24-26, 2011.
13. Thorvaldsdóttir H, Robinson JT and Mesirov JP: Integrative Genomics Viewer (IGV): High-performance genomics data visualization and exploration. Brief Bioinform 14: 178-192, 2013.
14. Lam HY, Clark MJ, Chen R, Chen R, Natsoulis G, O'Huallachain M, Dewey FE, Habegger L, Ashley EA, Gerstein MB, *et al*: Performance comparison of whole-genome sequencing platforms. Nat Biotechnol 30: 78-82, 2011.
15. Wang Y, Addess KJ, Chen J, Geer LY, He J, He S, Lu S, Madej T, Marchler-Bauer A, Thiessen PA, *et al*: MMDB: annotating protein sequences with Entrez's 3D-structure database. Nucleic Acids Res 35 (Database issue): D298-D300, 2007.
16. Var view Protein 3D: https://www.ncbi.nlm.nih.gov/Structure/cblast/cblast.cgi?client=snp&master_gi=169234657&neighbor_gi=212374861.
17. Rinne T, Brunner HG and van Bokhoven H: p63-associated disorders. Cell Cycle 6: 262-268, 2007.
18. Berdón-Zapata V, Granillo-Alvarez M, Valdés-Flores M, García-Ortiz JE, Kofman-Alfaro S and Zenteno JC: p63 gene analysis in Mexican patients with syndromic and non-syndromic ectrodactyly. J Orthop Res 22: 1-5, 2004.
19. Zenteno JC, Berdón-Zapata V, Kofman-Alfaro S and Mutchinick OM: Isolated ectrodactyly caused by a heterozygous missense mutation in the transactivation domain of TP63. Am J Med Genet A 134A: 74-76, 2005.
20. Ianakiev P, Kilpatrick MW, Toudjarska I, Basel D, Beighton P and Tsipouras P: Split-hand/split-foot malformation is caused by mutations in the p63 gene on 3q27. Am J Hum Genet 67: 59-66, 2000.
21. Rinne T, Hamel B, van Bokhoven H and Brunner HG: Pattern of p63 mutations and their phenotypes-update. Am J Med Genet A 140: 1396-1406, 2006.
22. Mangiulli M, Valletti A, Caratozzolo MF, Tullo A, Sbisà E, Pesole G and D'Erchia AM: Identification and functional characterization of two new transcriptional variants of the human p63 gene. Nucleic Acids Res 37: 6092-6104, 2009.
23. Gonfloni S, Caputo V and Iannizzotto V: P63 in health and cancer. Int J Dev Biol 59: 87-93, 2015.
24. Thanos CD and Bowie JU: p53 Family members p63 and p73 are SAM domain-containing proteins. Protein Sci 8: 1708-1710, 1999.
25. Enthart A, Klein C, Dehner A, Coles M, Gemmecker G, Kessler H and Hagn F: Solution structure and binding specificity of the p63 DNA binding domain. Sci Rep 6: 26707, 2016.
26. Stiewe T, Zimmermann S, Frilling A, Esche H and Pützer BM: Transactivation-deficient DeltaTA-p73 acts as an oncogene. Cancer Res 62: 3598-3602, 2002.
27. Yang A, Schweitzer R, Sun D, Kaghad M, Walker N, Bronson RT, Tabin C, Sharpe A, Caput D, Crum C, *et al*: p63 is essential for regenerative proliferation in limb, craniofacial and epithelial development. Nature 398: 714-718, 1999.
28. Vincek V, Knowles J, Li J and Nassiri M: Expression of p63 mRNA isoforms in normal human tissue. Anticancer Res 23: 3945-3948, 2003.
29. Koster MI, Dai D, Marinari B, Sano Y, Costanzo A, Karin M and Roop DR: p63 induces key target genes required for epidermal morphogenesis. Proc Natl Acad Sci USA 104: 3255-3260, 2007.
30. Koster MI and Roop DR: Mechanisms regulating epithelial stratification. Annu Rev Cell Dev Biol 23: 93-113, 2007.
31. Koster MI, Dai D and Roop DR: Conflicting roles for p63 in skin development and carcinogenesis. Cell Cycle 6: 269-273, 2007.
32. Sommer M, Poliak N, Upadhyay S, Ratovitski E, Nelkin BD, Donehower LA and Sidransky D: DeltaNp63alpha overexpression induces downregulation of Sirt1 and an accelerated aging phenotype in the mouse. Cell Cycle 5: 2005-2011, 2006.
33. Yan W and Chen X: GPX2, a direct target of p63, inhibits oxidative stress-induced apoptosis in a p53-dependent manner. J Biol Chem 281: 7856-7862, 2006.
34. Restelli M, Lopardo T, Lo Iacono N, Garaffo G, Conte D, Rustighi A, Napoli M, Del Sal G, Perez-Morga D, Costanzo A, *et al*: DLX5, FGF8 and the Pin1 isomerase control ΔNp63α protein stability during limb development: A regulatory loop at the basis of the SHFM and EEC congenital malformations. Hum Mol Genet 23: 3830-3842, 2014.
35. Lo Iacono N, Mantero S, Chiarelli A, Garcia E, Mills AA, Morasso MI, Costanzo A, Levi G, Guerrini L and Merlo GR: Regulation of Dlx5 and Dlx6 gene expression by p63 is involved in EEC and SHFM congenital limb defects. Development 135: 1377-1388, 2008.